SciencePG
Science Publishing Group

Analysis of Landsat 8 Multispectral Satellite Imagery for the Identification of Rock-Based Archaeological Sites in India

Bhooma Srinivasan[1], Friedrich Teichmann[2, *]

[1]Department of Aerospace Engineering, University of Applied Sciences, Wiener Neustadt, Austria

[2]Geospatial Institute of the Austrian Armed Forces (Institut für Militärisches GeoWesen IMG), Vienna, Austria

Email address:

bhoomasrinivasan16@gmail.com (B. Srinivasan), friedrich.teichmann@fhwn.ac.at (F. Teichmann),
friedrich.teichmann@bmlvs.gv.at (F. Teichmann)

[*]Corresponding author

Abstract: Despite the fact that highly intriguing, historical and world famous architectures are all carved out of rocks or made up of stones, there has been a continuous vacuum in the academic literature for the stone artefacts that requires investigation regarding the spectral response curve or a specific bandwidth to identify structures made up of rocks. Therefore, this research throws some light on the rock-cut caves and sculptures which stand as a heritage monument in many places in and around India by incorporating the multispectral Landsat satellite imagery. This paper aims to corroborate a methodology to find rocks using a discrete Landsat satellite band that would highlight rock based structures from various land cover backgrounds retrieved by multispectral remote sensing methodology. Four different non-examined and two well-known archaeological sites are taken as case studies to analyze and average across the study area samples for best results. Withal it is essential to understand that this research outcome will provide a comprehensive overview of the interesting observations obtained by Landsat satellite imagery with comparatively limited spatial resolution.

Keywords: Multi-spectral, Remote Sensing, Archaeology, Photogrammetry, Rocks, Spectral Signature

1. Introduction

Satellite images are generally captured using sensors and digital technology. Also, the prelude of infrared false color films has engendered a paramount shift in results, refining analysis by conventional analogue photo-interpretation techniques. The remote sensing techniques in the archaeological field are influenced by sensors capable of extending data acquisition in the electromagnetic spectrum by detection and measurement of radiation of different wavelengths reflected or emitted from distant objects. In addition, utilizing multi-spectral imaging, one can visually perceive features that the human ocular perceiver is not capable of detecting but still limited with respect to hyperspectral imagery which can show distinct difference between three different minerals, unlike multispectral imagery. This avails the archaeologists to extract increasingly abundant and involute information from the archaeological remains.

2. Background

2.1. Archaeological Excavations Using Multispectral Imagery

In reference to the field of remote sensing archaeology and image interpretation, umpteen number of archaeological explorations has been conducted using the multispectral and hyperspectral imageries. Since our research interest is based on the multispectral remote sensing archaeology, there are quite a few instances listed below with similar kind of work with respect to potential sites unearthed by multispectral imagery, such as the following:

Mexico: A Mexican archaeologist named Bill Middleton excavated Oaxaca, the southern state of Mexico using multispectral imagery provided by the Earth Observing 1 and Landsat satellites and with the implementation of the image processing techniques to tease the information from the imagery. This environmental change detection technique

works based on the different absorption and reflective patterns of the various features such as plant species, ecosystems etc. that are not perceived in the visible light but are identified when sampled against various portions of the electromagnetic spectrum [1].

Egypt: 17 lost and potential buried pyramids as well as more than 1,000 tombs and 3,100 antiquated settlements have been found using infrared satellite pictures, by an Egyptologist named Dr. Sarah Parcak [2]. She gathered the evidence that evinced hundreds of dwellings and a map, more of a blueprint of one of Egypt's most important capitals at the 3,000-year-old city of Tanis that has buildings, streets, admin complexes and houses [3]. Sarah Parcak employed various strategies to comprehend past human environment and ancient settlement locations to uncover the buried truth in Egypt. These analysis techniques involve computer algorithms and adding colors to farmland, urban, vegetation, water and archaeological sites [4].

Mexico: In the jungles of north-eastern Guatemala, a pristine 2,000-year-old mural, identified as the Maya maize god which spanned nearly 60 feet [3] was unearthed by Dr. Saturno with the help of high resolution IKONOs multispectral satellite data and the discolorations next to the silhouette of the architectural site were disclosed by the remote sensing techniques.

Mexico: William Gadoury, a 15-year-old Canadian schoolboy unearthed the lost Mayan cities concealed in the jungles, with the help of satellite imagery. He also claims to have found the relation between 22 constellations and 117 Mayan cities dispersed in different directions throughout Mexico, Guatemala, Honduras and El Salvador [5] [6].

It is intriguing to look into these past works documented by accredited researchers with substantive findings in unearthing archaeological sites at various locations in the world and is the major driving force behind this research paper.

2.2. Spectral Signatures

An underlying basis behind the remote sensing technique and the spectral interpretation is the ability to measure the reflected energy from different materials over a larger landscape. The spectral reflectance measured as a function of wavelength [7] is the ratio of reflected to incident radiation. The reflectance of each landscape feature falls between 0% and 100% reflectance in the electromagnetic spectrum. The no reflectance region happens to fall in the 0% and the 100% reflectance occurs when the sensor captures all the light reflected from the feature. These reflected electromagnetic radiation that travels in waves, when recorded and measured at different wavelengths and at discrete portions on a broader spectrum, results in the "spectral signature" that can be used to differentiate each object from its surroundings [8] [9].

Spectral patterns are produced by fundamental differences in the capacity of surface materials to absorb, reflect and emit radiant energy. Each land cover, say water, cultivated soil, vegetation, or minerals, each have distinctive spectral curves. But these spectral curves can alter over a period of time and therefore the visual cues and context of interest are crucial factors for qualitative judgements to inspect the suitable spectral region [10].

The vegetation, soil, water and minerals are the broad classes of Earth surfaces that are predominantly found in the spectral response curve archives. Oodles of detailed study has been done in the literature on the spectral signatures of the broadly classified following landcover classes.

Vegetation: Vegetation interacts with light in a different way than other natural material. The vegetation spectrum absorbs in the red and blue wavelengths, reflects in the green wavelength, and strongly reflects in the near infrared (NIR) wavelength. The percentage of reflection is about 9% in the red region 4% in the blue region, 15% in the green region and 42% in the near infrared region [11]. The spectral reflectance of the plants is significantly influenced by two principal parameters namely, chlorophyll and the water content in the leaves [12]. The more leaves a plant has, the more the wavelengths of light are affected. The vegetation spectral signature can say more about the type or health of the vegetation. For example, the dry grass has higher reflectance in the visible region but lower reflectance in the NIR region [13]. Different plant materials, water content, pigment, carbon content, nitrogen content, and other properties cause further fluctuations across the spectrum.

Soil: The spectral reflectance of the soil curve is quite complicated because of the composition of soil. The soil composition is uncovered in the thermal bands because of the temperature variations of structures present beneath it [10]. The soil dampness is a highly influencing parameter when studying the spectral response curves. The moisture present in the soil is inversely proportional to spectral reflectance and hence affects the response curves. The response curves are low in reflectance in the regions of high moisture. This is very helpful in studying about the buried structure [14]. Similar to the soil moisture, the presence of vegetation is an affecting factor. The density of vegetation builds up in the soil with vegetal covering, with the raise in humidity. Whereas wet soil absorbs radiance in the near infrared in the absence of vegetal covering, because of the obscurity typical of water. The difference in the reflectance level is around 1.4 μm when the reflectance value of dry soils increases from blue to near infrared, while reflectance value of wet soils decreases from red to infrared [11].

Water: Water normally reflects high in the visible spectrum and increasingly absorbs the light in the NIR leaving the water to appear dark [7] [10]. The spectral reflectance of the water is affected by the inorganic materials present in the water bodies. The more the inorganic materials, the more chances are for the shift in peak reflectance towards red region from the green region of the spectrum. However, the clearer water has less reflectance than turbid water.

Minerals: The chemical composition of hydrogen and carbon ions play a major role in studying the mineral spectral curves as the as the reflectance and absorption patterns change based on the presence of these ions in the respective minerals [15]. Therefore, different kind of minerals shows significant

absorption in different regions. Notable absorption of hematite is in visible region, calcite is between 1.8 and 2.4 µm, kaolinite is in 1.4 µm and orthoclase feldspar is from visible to middle infrared [15]. The short-wave infrared has shown potentials in detecting the hydroxyl bearing minerals [9].

The spectral response curves have been studied for the sedimentary rocks using hyperspectral imagery [16], but very little has been spoken about the spectral importance of rocks in general using multispectral imagery. In most cases, is often consolidated with the spectral signatures of minerals because the rocks are basically made up of a combination of minerals [10]. In other words, the spectral response curve of any rock corresponds to the spectral signature of its constituent mineral [17]. Per remote sensing literature, spectral bandwidths of these constituent minerals of the rock tends to fall between 0.6 to 2.5 µm which is referred to as the short-wave infrared [10] [12].

3. Research Aim

This research aims to provide a tool to assist rock based archaeology by incorporating satellite remote sensing techniques by detecting the rock based structures with the multispectral low resolution Landsat satellite imagery. This improves the efficiency of the archaeological explorations in unveiling anomalies with regard to natural rock outcrops or man-made rock based sculptures. The following are the sub-classifications to the research question in order to arrive at the desired research outcome.

a To find the spectral signature for the rocky structures, a unique pattern owned by each land cover.

b To find the specific spectral band that can purely highlight the rocks against any other land cover backgrounds.

4. Methodology

4.1. Study Areas

In order to understand and compare the bandwidths better, the Landsat image (low resolution data) of the four study sites that are of archaeological interests in India and the two studied well-known sites are collected and the relative effectiveness of both the data results are studied. The satellite remotely sensed data was acquired from the Landsat 8 archive which is available as an open source for the satellite images.

The focus of the study are the archaeological sites depicted below in the World map (figure 1), collectively, and separately in the respective state maps (figure 2).
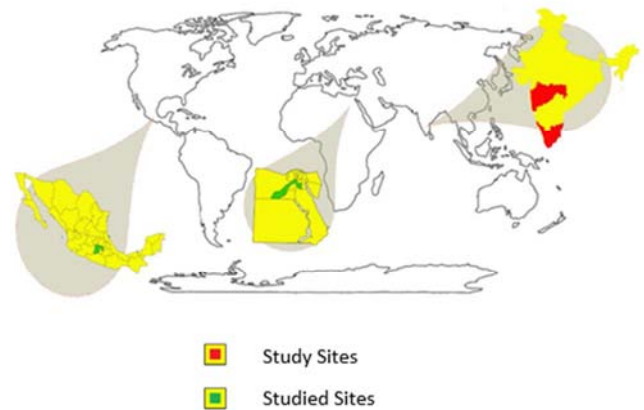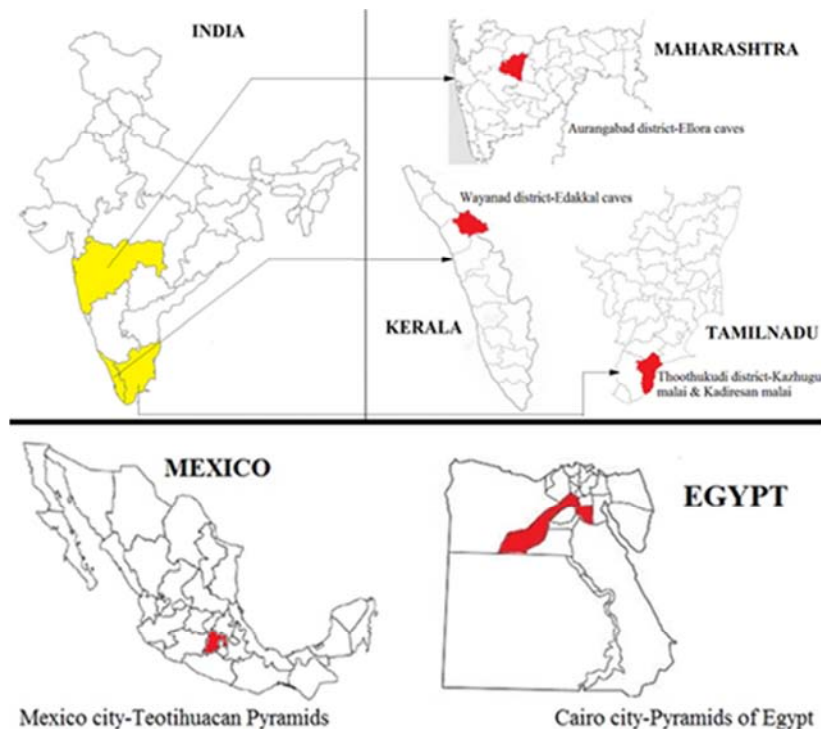

Figure 1. World Map with Areas of Interest.

Figure 2. Country and State Maps with Areas of Interest.

4.1.1. Study Sites

Kazhugu Malai: Kazhugu malai, when literally translated means the mountain with inhabitants of Eagles, is a small village located about 50 km inland from the Thoothukudi port in the state of Tamil Nadu. It is geographically positioned at 9°9'10"N, 77°42'15"E and is a place of archaeological importance with the rock-cut sculpture and carvings dating back to 8th century A. D, built during the ruling period of Pandya Kings. This is the only architecture of the Pandya kings still surviving. The kazhugu malai is a jaw dropping experience as the sculpture is made up of a monolithic rock, 25ft deep and the architectural details in the carvings of rock-cut sculptures holds a greater significance with each line in the carvings owning a meaning.

Figure 3. *Kazhugu Malai.*

Kathiresan Malai: The Kathiresan malai is a natural cave outcrop and entrance to the cave is a small opening. When one crawls through it, can find a startled scene which is quite spacious and identical to a football ground. The cave is lighted by sunlight which peeps in through a small hole and brightens the entire interior part of the cave. The specialty is that it is said, the fine granules of sand shines gold through the beam of light that torches the cave. Due to social security and safety the entrance to the cave is prohibited. One must obtain permission from the local bodies governed by the Government of India as it comes under the archaeological survey of India.

Figure 4. *Kadiresan Malai.*

Eddakal Caves: The Edakkal caves are geographically located at 11°37′28.81″N, 76°14′8.88″E and are situated at Edakkal, 25km from Kalpetta and 1,200m above the sea level on Ambukutty Mala in the Wayanad district of Kerala. The name "Edakkal", when literally translated means "the stone in between". The formation of the cave, a fissure which was created due to natural changes which is 22 feet in width and 96 feet in length of split in the rock and the depth of the cleft extends to over 30 feet with a large rock forming a roof over it.
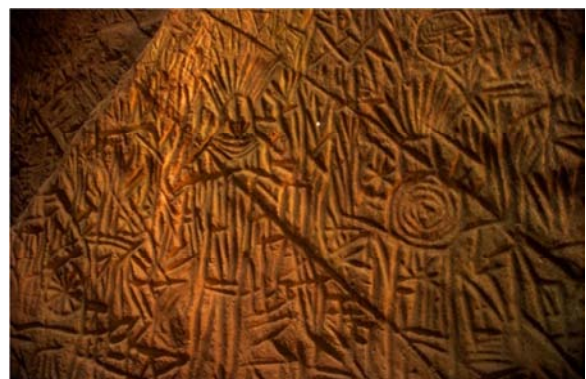

Figure 5. *Edakkal Caves [18].*

Ellora Caves: Ellora caves are geographically located at 20.0238°N, 75.1793°E. This UNESCO World Heritage site is one of the largest rock cut architecture situated 29 km north-west of the city of Aurangabad in the Indian state of Maharashtra. The Ellora caves stretches to about 2km and houses about 34 caves comprising various monasteries and temples dug side by side, dating back to a period between 5th and 10th century during the period of Rashtrakuta king Krishna I. As seen in other rock cut architectures, the Ellora caves also holds multi-religious sculptures and carvings such as Buddhism, Hinduism and Jainism etc.

Figure 6. Ellora Caves [19].

4.1.2. Studied Sites

The studied sites include the "Pyramids of Egypt" and "Teotihuacan" geometrically positioned at 29.9792° N, 31.1342° E and 19.6923° N, 98.8435° W respectively. The pyramids of Egypt and Mexico were chosen for referencing or standardizing the data as they are well-known, gigantic and therefore easy to delineate the geographic boundary, covers a good band sample for rock patterns because they are not covered with vegetation unlike the ones taken for study areas.

4.2. Data Download

The Landsat images were obtained from the USGS Earth Explorer "earthexplorer.usgs.gov" which is one of the largest databases of remote sensing data with user friendly interface allowing the users to:

a Download data over chronological timelines

b Wide range of search criteria specifications and

c A long list of satellite and aerial imagery to choose.

The interface of Earth Explorer is based on google maps with tab operations. The initial step towards the data download was to search the catalogue with options to create a scene of interest by coordinates, by feature search (river, castle, church etc.), by importing spatial file, by timeframe search through a long list of acquisitions to find the correct date of the image, etc. In this case the area of interest was geographically located with the coordinates.

Then a list of different satellite image and aerial imagery archive appears from which the Landsat 8 OLI was picked as the data set of choice. The search results provide the populated results of the interested search area with the image preview of the AOI with different data acquisition date, rows and path values, entity Id or the scene information, coordinates that highlights different scenes. The refining of the image can be done by selecting a series of criteria such as in this case was low cloud coverage, recent and good quality image. In some cases, the recent image can contain high cloud covering over the AOI and hence a month old or a much older image had to be considered.

4.3. Data Product

The downloaded data comprises of 13 files that includes the 11 band, 16 bit GeoTIFF images, a metadata file, and a quality assessment image. The 11 band images include 9 multispectral bands from the OLI and the two thermal images from the thermal infrared sensor. Each spectral band image is a 16bit greyscale image. The metadata file comprises of spatial information and the parameters to identify the scenes. The quality assessment data hold the quality statistics and the cloud information of the data product. The QA image can be stretched to enhance the light and dark pixels to check for the image quality.

4.4. Data Processing

4.4.1. Erdas Imagine

The satellite image, which is made up of raster graphics, was imported to a remotely sensed data reader and editor known as Erdas Imagine developed by the Hexagon Geospatial. It makes the raster images more understandable with varied options for processing the needs of all the geospatial applications such as remote sensing, photogrammetry and geographic information system.

4.4.2. Layer Stack

The downloaded satellite image is the raw image and is generally a collection of bands, provided to the user as individual separate bands in the form of tiff format. Each band is in grey scale, that is, black and white and the color image, which is a combination of three different bands, is the output of the layer stacking procedure. The layer stacking was performed by combining the bands provided only by the Landsat 8 OLI sensor and leaving out the thermal bands provided by the TIRS.

4.4.3. Subset

The layer stacked image was truncated based on the area of interest. This is important when only a part of the image is needed for the analysis. To accomplish the subset image two things are necessary, namely the AOI boundary file and the main satellite image should be geo-referenced and both are required to be in the same co-ordinate system.

4.4.4. Signature Set

These raster graphic images of each areas of interest were converted into signature sets or training samples, which are nothing but the mean digital numbers to classify the images. Each of these signature sets of known identities are used to classify similar characteristics of pixels of unknown identity. The mean of these signature sets results in the signature mean plot with the mean values of the spectral reflectance of the feature against the band layers in the image.

4.4.5. Feature Space Images

Withal, the feature space images were plotted, a set of instances which are represented by dots in the scatter plot that corresponds to certain features. The feature space images were plotted for all the bands in the Landsat satellite but in a combination of two, to specifically analyze each combination that highlights a specific landcover and its corresponding bandwidths.

5. Results and Discussion

The curves are brought together to visually understand the variations in their behavioral pattern and differences in the percentage of reflectance measured at discrete portions of the electromagnetic spectrum and plotted across different spectral bands of the Landsat 8.

5.1. Signature Plots

The figure 7 conspicuously proves that the spectral reflectance is at the maximum in the band number 6, the shortwave infrared in the Landsat 8, whose wavelength ranges between 1.57 and 1.65μm. Furthermore, the graph delineates the average or the minimum spectral reflectance of the rock based structures in the AOIs. The percentage of reflectance ranges between 82 and 92 for the band 6 to highlight the rocky features. The average curve of the mean signature plot serves as the spectral signature of the rocks.
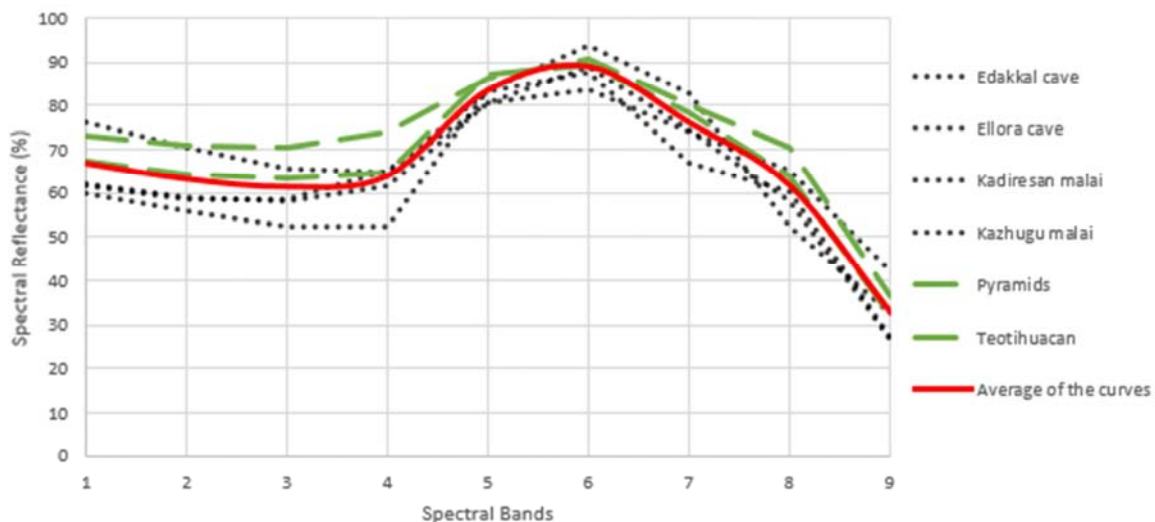

Figure 7. *Average of Signature mean plots.*

5.2. Summary of Spectral Signatures

A comparative study has been done with the spectral signature of rocks and other land covers from the literature [7] [9] [10]-[17]. The figure 8 below illustrates how the four curves are almost spaced close in the visible region (0 to 0.7 μm) which explains the fact that the spectral reflectance of vegetation, soil and water are similar in that region and the rock shows potential reflectance in the red light of the visible spectrum. To discriminate these land covers more precisely and distinctly, it is indeed essential to consider the longer wavelengths of the electromagnetic spectrum.

Spectral reflectance of Vegetation, water and soil: The spectral reflectance of vegetation seems to have the least reflectance value in the red and blue regions of the visible portion (0 to 0.7 μm) of the electromagnetic spectrum because they absorb the visible light whereas reflect in the near infrared and hence the curve dramatically increases in the near infrared (0.7 to 1 μm). But when examined closely vegetation has the low visible reflectance compared to other land covers. The water graph is characterized by a high reflectance in the visible region and extensive absorption at the longer wavelengths other than the visible region of the electromagnetic spectrum. It also is potentially highlighted in the near infrared due to the presence of inorganic substances. The soil curve shows uniform increase from the red region of the visible spectrum and varies conspicuously along the longer wavelengths of the spectrum due to various compositions of soil and the presence of external features, example buried structures.
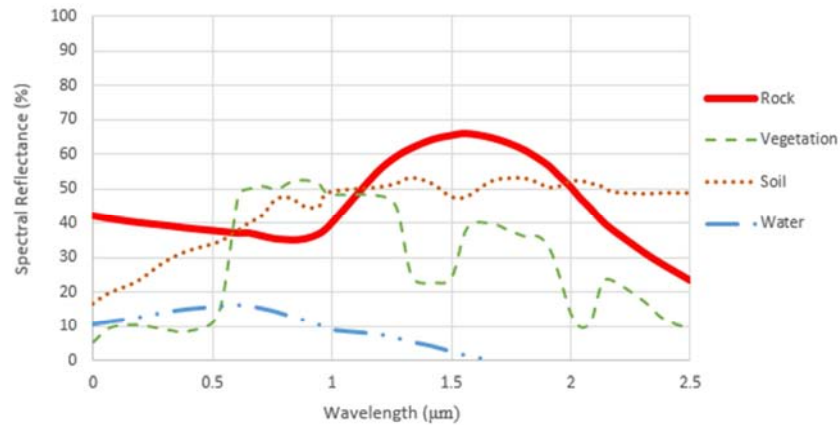
Figure 8. *Spectral Signatures of rock, vegetation, soil and water.*

Spectral reflectance of Rock: Similar to soil, the rocks also have different compositions and always have interference from the vegetation. As previously stated, since the vegetation reflects near infrared, the spectral signature of the rock also gradually increases from the near infrared region towards the short-wave infrared. But unlike the other curves, the rocks reflect both in the visible and the mid infrared regions. The reflectance in the red region in the visible spectrum is high comparative to the other land covers and gradually decreases through the green and blue regions of the visible spectrum. The spectral reflectance in the red region is about 41% and this could possibly be because of the presence of high concentrations of iron or iron oxides, since the red light of the visible spectrum can aid in recording these minerals. As the curve progresses, there is a minor dip at the beginning of the near infrared region of the electromagnetic spectrum due to the possible presence of water as the water absorbs near infrared. The curve dramatically increases towards the short-wave infrared region ranging between 1.57 μm and 1.65μm, and the curve stays consistently stable with the maximum reflectance throughout the SWIR region in these intervals. Further, the curve gradually decreases in the longer wavelengths of electromagnetic spectrum which in other words are absorbed by the rocks.

The reasons behind the maximum reflectance and the consistency throughout the SWIR region are discussed below.

  a The areas of interest at which the curve was plotted can have the substance of moisture present in the rock and hence can reflect extensively at the shortwave infrared region.

  b The water gauged in the rock can possibly reflect more at the shortwave infrared region.

  c The areas of interest, the rocks, may exhibit smoldering effects and can contribute to the maximum reflectance in the shortwave infrared region.

  d The minerals present in the rock compositions can also reflect more in the shortwave infrared region.

5.3. Feature Space Images

The scatter plots were used to emphasize more on the SWIR band 6. The scatter plots of, especially, band 4 vs band 6 are considered in order to highlight the vegetation vs rocks since the pixel intensities of vegetation and rock were more or less the same with slight fluctuations in the values in some of the spectral profiles. This is because as most of the rocks in the AOIs are surrounded by different kinds of vegetation.

The ellipses in the graph comprises of 99% of the pixels of a specific class, say for example rock or vegetation, etc. Therefore, depending upon the clusters of dots inside the ellipses, the density of pixels and effect of the corresponding land cover classes can be determined. The pixels for the rocks are inside the brown colored ellipses in all the graphs and are at the highest points in the graphs, meaning stone artefacts reflects most of wavelength in band 6. The overlapping of ellipses is due to the standard deviation value and also, because of potential plant growth on the rocks.
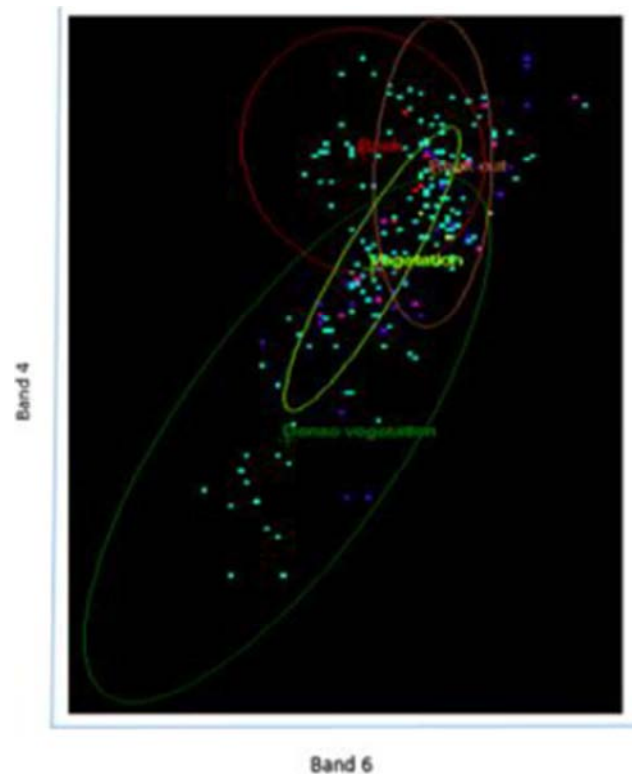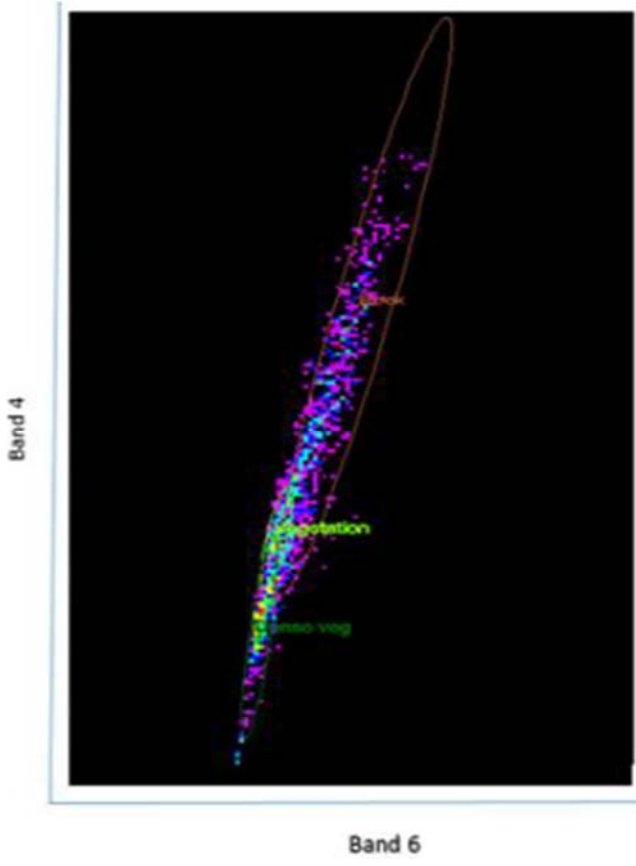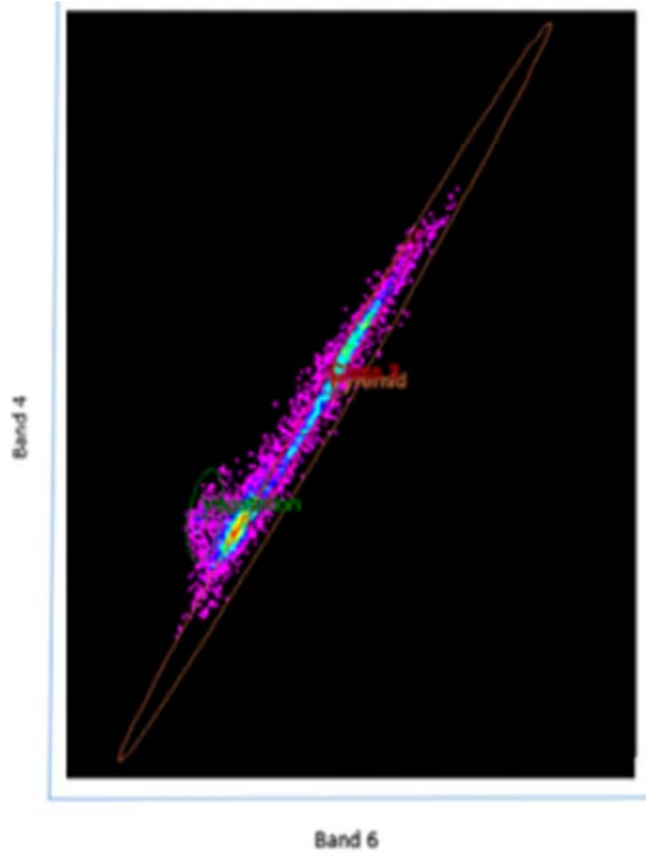

Figure 9. *Kazhugu Malai.*

Figure 10. *Edakkal Caves.*

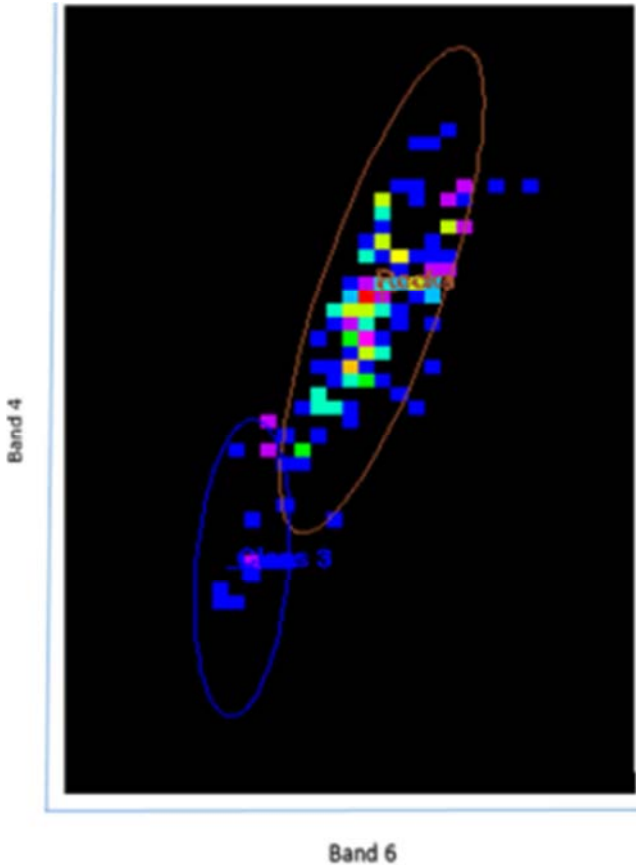***Figure 12.*** *Pyramids of Egypt.*

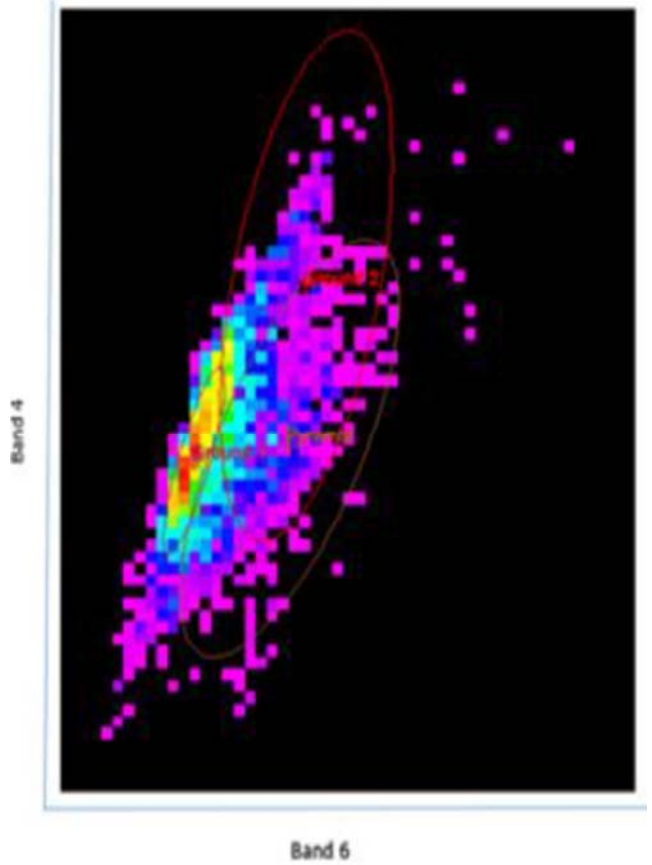***Figure 11.*** *Ellora Caves.*

Figure 13. *Teotihuacan.*

6. Conclusion

With all garnered results, a methodology to reveal the rock-based features in a satellite imagery using low resolution multi-spectral Landsat imagery to enhance the efficacy of archaeological prospections has been successfully derived. This research paper has answered the valid individual spectral bands and corresponding bandwidths, solely for the identification of rocks which were the "missing delta" in the literature review [7] [9] [10]-[17].

It is possible to classify each pixel of the image into different spectral categories defined by its spectral signature. This unique spectral signature for the rock based structures showed maximum percentage of reflectance ranging between 82 and 92 for the corresponding spectral band 6, attained between the wavelengths 1.57 and 1.65μm corresponding to the spectral band 6 f the Landsat-8 spectral bands. The significance of the spectral signature plot of the rock is that it can be used to check for similar signatures when performing any rock based analysis.

The regional knowledge integrated with the satellite imagery and remote sensing image processing techniques have enhanced the understanding of the pixel based classification procedures corroborating and assisting the innovative methodology that has been the key research of this paper.

References

[1] S. Gawlowicz, "NASA Landsat Science," 16 05 2008. [Online]. Available: https://landsat.gsfc.nasa.gov/archaeologist-uses-landsat-to-explore-ancient-mexico/. [Accessed 09 03 2017].

[2] "National Geographic Society, "Sarah Parack, Archaeologist"," [Online]. Available: http://www.nationalgeographic.com/explorers/bios/sarah-parcak/. [Accessed 09 03 2017].

[3] M. Petronzio, "Mashable "The New Golden Age of Archaeology Is Right Now"," 06 11 2013. [Online]. Available: http://mashable.com/2013/11/06/space-archaeology/#iZybcjuEuaqj. [Accessed 09 03 2017].

[4] M. Venkataramanan, "Wired.co.uk "Space archaeologist discovers lost cities with satellite imagery"," 14 11 2014. [Online]. Available: http://www.wired.co.uk/article/scanning-the-past. [Accessed 09 03 2017].

[5] "Star pupil finds lost Mayan city by studying ancient charts of the night sky from his bedroom," The Daily Telegraph, 10 05 2016.

[6] A. Willingham, "CNN "Breaking down the mythical 'Maya city' discovery"," 12 05 2016. [Online]. Available: http://edition.cnn.com/2016/05/11/americas/mayan-city-debunk. [Accessed 09 03 2017].

[7] X. Zhu, GIS for Environmental Applications: A Practical Approach, New York: Routledge, 2016.

[8] R. N. Clark, Manual of Remote Sensing, Remote Sensing for the Earth Sciences, New York, 1998.

[9] R. A. Ryerson and A. N. Rencz, "Spectroscopy of Rocks and Minerals, and Principles of Spectroscopy," in Remote Sensing for the Earth Sciences: Manual of Remote Sensing, John Wiley & Sons. Inc., 1999, pp. Pages 03-357.

[10] J. D. Bossler, Manual of Geospatial Science and Technology, CRC Press: Taylor & Francis Group, 2010.

[11] S. I. T. A. H. A. and H. I., "Archaeological prospection and remote sensing," Antiquity Publications Ltd, 1990.

[12] G. Joseph, Fundamentals of Remote Sensing, India: Universities Press, 2005.

[13] M. A. Ashraf, M. J. Maah and I. Yusoff, "Introduction to Remote Sensing of Biomass," Vols. 978-953-307-490-0, 2011.

[14] A. Rowlands and A. Sarris, "Detection of exposed and subsurface archaeological remains using," Journal of archaeological science, vol. 34, pp. 795-803, 2007.

[15] "Microimages: Introduction to Hyperspectral Imaging," [Online]. Available: http://www.microimages.com/documentation/html/Tutorials/hyprspec.htm. [Accessed 10 03 2017].

[16] F. F. Sabins, "Remote sensing for mineral exploration," Ore Geoglogy Reviews, vol. 14, pp. 187-183, 1999.

[17] F. F. Sabins, Remote Sensing: Principles and Applications, New York: W. H. Freeman & Co., 1997.

[18] "Edakkal caves," Kerala Tourism, 2013. [Online]. Available: https://www.keralatourism.org/destination/edakkal-caves-wayanad/335. [Accessed 17 05 2016].

[19] "Ellora Caves," UNESCO World Heritage Center, [Online]. Available: http://whc.unesco.org/en/list/243/gallery/. [Accessed 17 05 2016].

[20] C. Bassani, R. M. Cavalli, R. Goffredo, A. Palombo, S. Pasucci and S. Pignatti, "Specific spectral bands for different land cover contexts to improve the efficiency of remote sensing archaeological prospection: The Arpi case study," Journal of Cultural Heritage, pp. 41- 48, 2009.